Accuracy of analytical theories for relativistic bremsstrahlung

D. H. Jakubassa-Amundsen*
Mathematics Institute, University of Munich, Theresienstrasse 39, 80333 Munich, Germany

A. Mangiarotti†
Instituto de Física da Universidade de São Paulo, Rua do Matão 1371, 05508-090 São Paulo, Brazil

(Received 8 May 2019; published 9 September 2019)

Angular and energy-dependent photon distributions emitted from 50-keV to 2.5-MeV electrons colliding with targets ranging from Cu to Pb are calculated using a consistent higher order analytical approach as well as the exact Dirac partial-wave theory. By comparison with exact numerical results for neutral atoms, the validity of the Olsen-Maximon-Wergeland additivity rule for handling the screening correction is probed, and its applicability for collision energies above 100 keV, if the photon frequency and emission angle are both small, is established. The comparison for a point-Coulomb field, aimed at testing the accuracy of the underlying analytical theory, reveals in most cases a deviation below 60% for Au, decreasing with target nuclear charge down to 10–20% for Cu.

DOI: 10.1103/PhysRevA.100.032703

I. INTRODUCTION

When an electron traverses a given material, it may lose equal amounts of its energy to ionization and radiation emission [1]. The collision energy $E_{\rm crit}$, where this happens, ranges typically from several tens of MeV for C to a few MeV for Pb. Hence, it is clear that accurate bremsstrahlung cross sections are of paramount importance to describe the interaction of electrons with matter around $E_{\rm crit}$ or above. In other cases, which are focused on radiation emission, like the generation of x rays with electron tubes or plasma focus devices, the knowledge of bremsstrahlung cross sections is fundamental for energies even much below $E_{\rm crit}$. Taken all together, such diverse fields as the simulation of the interaction of particles with detectors, the interaction of cosmic rays with the atmosphere, medical physics, and the generation of terrestrial γ-ray flashes in thunderstorms are in need of these fundamental data.

Only nuclear bremsstrahlung will be considered here because it is the dominant process for all elements except the lightest ones. From the point of view of fundamental physics, nuclear bremsstrahlung is one of the simplest interaction mechanisms between an electron and an atom involving the coupling to the radiation field. Essentially, it is the radiative version of elastic scattering, to which it is related by the low-energy theorem. First calculations were performed more than 80 years ago, at the dawn of quantum electrodynamics, by Sommerfeld in 1931 [2] for nonrelativistic electrons and by Sauter [3], Bethe and Heitler [4,5], and Racah [6] in 1934 for relativistic electrons. These formulations, employing the plane-wave Born approximation (PWBA), are inadequate for meeting the quantitative demand of modern applications. PWBA results can be incorrect by even an order of magnitude at large angles, and they are incapable of giving a nonzero value of the cross section at the short-wavelength limit of the photon spectrum. Despite the large progress over the past 50 years, it is still impossible to calculate bremsstrahlung cross sections accurately from 1 keV to 1 TeV with a single approach. Instead, a patchwork of different methods with different accuracies is in use. There are two main reasons for this dilemma. One is the need to account for both the distortion of the wave function of the projectile electron close to the nucleus, which renders the PWBA incorrect as discovered by Bethe and Maximon in their seminal work [7], and for the screening effect of the atomic electrons. The other reason is the impossibility to express the scattering states of a relativistic electron for a point-Coulomb field in closed form, which is in contrast to the nonrelativistic Schrödinger case. Only approximate analytical solutions to the Dirac equation, the Sommerfeld-Maue (SM) wave functions [8], are known to date.

An exact method for nuclear bremsstrahlung was pioneered in the 1970s by Pratt and coworkers [9], which, nevertheless, needs numerical computations. It is based on the expansion of the Dirac wave functions of the electron in a realistic atomic potential in terms of partial waves (DW). However, for initial energies of the electron beyond a few MeV, low photon frequencies (below some 10% of the collision energy), and photon emission angles close to the forward direction, the number of terms contributing to the cross section can exceed a million. Although the DW theory is accurate per se, it is beyond its reach to obtain reference cross sections above tens of MeV for the full radiated spectrum. As a matter of fact, this type of approach was pushed to its limits in our previous work [10] by using the Olsen-Maximon-Wergeland (OMW) additivity rule [11] to calculate the spectral distribution of the emitted photons for unobserved final electrons. This rule relies on the separability of the Coulomb distortion

*dj@math.lmu.de
†alessio@if.usp.br

(which is important at high momentum transfers, i.e., $q \gtrsim m_e\, c$, respectively small distances, where the electron gets close to the nucleus) from the screening (which occurs predominantly at low momentum transfer, $q \ll m_e\, c$, respectively large distances, where the distortion by the central field is weak). Therefore, the distortion and screening effects can be treated in an additive way when calculating the bremsstrahlung intensity. It was then possible to reach 10 MeV and to obtain results for a major part of the radiated spectrum by using a highly optimized code for the case of a point-Coulomb field, where the solutions of the Dirac equation possess an asymptotic representation in terms of Whittaker functions [12]. This asymptotic representation is much easier to handle numerically above a few MeV (or at the foremost angles) than the Bessel function asymptotics in the case of a neutral target. We note that the OMW prescription was not only used in our previous work but it is in fact the basis of the most accurate analytical results.

Above 10 MeV, only analytical calculations are possible for a large part of the radiated spectrum. Therefore, a detailed study of their validity is of great interest. In the analytical description of bremsstrahlung, basic progress was made by introducing the Sommerfeld-Maue wave functions instead of plane waves. This leads to an improvement since the distortion by the central field is treated in a better way but can be applied only to the point-Coulomb case, thus neglecting screening. The resulting SM theory was first applied to bremsstrahlung by Bethe and Maximon [7]. Their work is still the basis for the identification of those matrix elements which contribute to leading order (LO) in $\alpha\, Z$ (where Z is the nuclear charge number of the target and α is the fine structure constant) to the cross section, a nontrivial task in the SM theory. However, their expression for the cross section was obtained in the ultrarelativistic (i.e., $E_i \gg m_e\, c^2$ and $E_f \gg m_e\, c^2$) and small-angle limits. The complete result without these approximations was first published by Elwert and Haug [13]. It is a relativistic theory which is exact up to first order in $\alpha\, Z$ for the radiation matrix element (i.e., second order for the cross section). We recall that the SM wave functions are accurate: (i) when $\alpha\, Z \ll 1$ or (ii) at high energies and large distances from the origin of the central field. Because the analytical approach is limited to the point-Coulomb case, screening must be taken into account in a separate step via the OMW additivity rule.

In order to improve on this leading-order Sommerfeld-Maue (LO-SM) approach, a next-to-leading-order (NLO) approximation to the initial and final wave functions of the electron was introduced by Roche and coworkers [14], which is accurate up to second order in $\alpha\, Z$. In the high-energy limit, the respective wave functions can be represented in a way that leads to a closed form for the correction to the cross section. In their resulting theory, which will be termed NNLO-SM, Roche *et al.* [14] included also one extra term of the next-to-next-to-leading-order (NNLO), justifying it by an improved agreement with experimental data. This practice was later followed by all published works on that topic, to the best of our knowledge (see, e.g., the review by Mangiarotti and Martins [15] and a follow-up paper [10]).

The main goals of the present paper are twofold. One is to probe the OMW additivity rule by comparing its results to those from a DW theory where screening is fully accounted for. To this aim, we consider collision energies between 100 keV and 1 MeV, which is a region where the OMW additivity rule can be checked effectively. The other goal is to introduce and to test an alternative approach, termed NLO-SM theory, which is consistent in orders of $\alpha\, Z$. It is defined without the pathological NNLO contribution, which was recently found to lead to severe errors, at least in some cases, for backward photon emission (see the conference proceedings [16]). This testing can only be achieved by a comparison with DW results, because currently available experimental data are too scarce and inaccurate (the uncertainties being of the order of 10%) to serve such a purpose [17]. As demonstrated below, a large improvement of the correction to the leading order at backward photon angles is found and much better results can be obtained for bremsstrahlung cross sections at a few MeV by analytical means than previously thought possible.

The paper is organized as follows. Section II gives an outline of the analytical approach and of the DW theory. Screening effects as a function of collision energy are investigated in Sec. III for Sn, Au, and Pb targets, including the test of the OMW additivity rule against the screened DW theory. In Sec. IV, results for the photon spectra are given within the analytical theory in comparison with experimental data and DW results for targets ranging from Cu to Au. The conclusions are drawn in Sec. V. Atomic units ($\hbar = m_e = e = 1$) are used unless indicated otherwise.

II. THEORY

In our theoretical approaches, the photon field is treated to first order, a commonly used approximation for collision energies up to the MeV region. Accounting for undetected scattered electrons and unobserved polarization degrees of freedom, the doubly differential cross section for the emission of bremsstrahlung with momentum $\boldsymbol{k}$ and frequency $\omega = c\, k$ into the solid angle $d\Omega_k$, is given by [18]

$$\frac{d^2\sigma}{d\omega\, d\Omega_k} = \frac{4\pi^2 \omega\, k_f\, E_i\, E_f}{c^5\, k_i}\, \frac{1}{2} \sum_{\sigma_i,\sigma_f} \sum_{\lambda} \int d\Omega_f\, |W_{rad}|^2, \quad (2.1)$$

where the triply differential cross section for the elementary process of bremsstrahlung is integrated over the final solid angle $d\Omega_f$ of the electron, summed over its spin projection σ_f as well as over the two linear polarization directions λ_1 and λ_2 of the photon, and averaged over the initial spin projection σ_i of the electron. The radiation matrix element is defined by

$$W_{rad} = \int d\boldsymbol{r}\; \psi_f^{(\sigma_f)\dagger}(\boldsymbol{r})\; (\boldsymbol{\alpha} \cdot \boldsymbol{e}_\lambda^*)\; e^{-i\boldsymbol{k}\cdot\boldsymbol{r}} \psi_i^{(\sigma_i)}(\boldsymbol{r}), \quad (2.2)$$

where $\boldsymbol{\alpha}$ is the vector of Dirac matrices. In Eq. (2.1), $\boldsymbol{k}_i$, $\boldsymbol{k}_f$ and E_i, E_f are, respectively, the momenta and total energies of the initial and final states of the electron.

The approaches introduced below differ in the choice of the wave functions ψ_i and ψ_f, which describe the scattering electron. On one hand, they are exact solutions to the relativistic Dirac equation and are expressed as a sum of partial waves. In this DW theory, the electron-target atom interaction is either described by a central static screened potential or by a point-Coulomb field. On the other hand, ψ_i and ψ_f

are approximated by the analytical Sommerfeld-Maue wave functions valid only for a point-Coulomb potential.

A. Analytical approach

In the analytical approach, the treatment of the static atomic potential $V(r)$ proceeds in two steps. In the first step, $V(r)$ is replaced by a point-Coulomb field, $V_{\rm Coul}(r) = -Z/r$. In the leading-order Sommerfeld-Maue (SM) approximation, $\psi_{\rm i}$ and $\psi_{\rm f}$ are represented by SM wave functions. For an incoming electron, this wave function reads

$$\begin{aligned}
\psi_{\rm i}^{{\rm SM}(\sigma_{\rm i})}(\boldsymbol{r}) &= \psi_{\rm a}^{{\rm SM}(\sigma_{\rm i})}(\boldsymbol{r}) + \psi_{\rm b}^{{\rm SM}(\sigma_{\rm i})}(\boldsymbol{r}),\\
\psi_{\rm a}^{{\rm SM}(\sigma_{\rm i})}(\boldsymbol{r}) &= N_{\rm i}^{\rm SM}\, e^{i\boldsymbol{k}_{\rm i}\cdot\boldsymbol{r}}\; {}_1F_1(i\,\eta_{\rm i},\,1,\,i(k_{\rm i}r - \boldsymbol{k}_{\rm i}\cdot\boldsymbol{r}))\, u_{k_{\rm i}}^{(\sigma_{\rm i})},\\
\psi_{\rm b}^{{\rm SM}(\sigma_{\rm i})}(\boldsymbol{r}) &= -N_{\rm i}^{\rm SM} e^{i\boldsymbol{k}_{\rm i}\cdot\boldsymbol{r}} \frac{ic}{2E_{\rm i}}\boldsymbol{\alpha}\cdot\boldsymbol{\nabla}\, {}_1F_1(i\eta_{\rm i},\,1,\,i(k_{\rm i}r - \boldsymbol{k}_{\rm i}\cdot\boldsymbol{r}))u_{k_{\rm i}}^{(\sigma_{\rm i})},\\
N_{\rm i}^{\rm SM} &= e^{\pi\,\eta_{\rm i}/2}\,\Gamma(1 - i\,\eta_{\rm i})/(2\pi)^{3/2},
\end{aligned} \tag{2.3}$$

where ${}_1F_1$ is a confluent hypergeometric function, $\eta_{\rm i} = Z\,E_{\rm i}/(k_{\rm i}c^2)$, Γ is the Γ function, and $u_{k_{\rm i}}$ is a free 4-spinor. In the next-to-leading-order SM approximation, an additional term $\psi_{\rm c}^{\rm RDP}$ is added to the SM wave function according to the prescription by Roche *et al.* [14]. No closed form can be obtained explicitly for $\psi_{\rm c}^{\rm RDP}$. However, in the high-energy limit, $\psi_{\rm c}^{\rm RDP}$ is defined implicitly, e.g., again for the incoming electron, by the solution of the equation

$$\left(\nabla^2 + k_{\rm i}^2\right)\psi_{\rm c}^{{\rm RDP}(\sigma_{\rm i})}(\boldsymbol{r}) = -\frac{(Z/c)^2}{r^2}\,\psi_{\rm a}^{{\rm SM}(\sigma_{\rm i})}(\boldsymbol{r}). \tag{2.4}$$

As shown by Roche *et al.* [14], Eq. (2.4) is sufficient to obtain a closed form for the corrections to the matrix element and hence to the cross section. When applying these modified wave functions to the calculation of the bremsstrahlung cross section, care has to be taken to retain consistently just those contributions which (a) survive in the high-energy limit and (b) are at most of third order in Z/c. To make this clear, the radiation matrix element is represented in the following form,

$$W_{\rm rad} = W_{\rm SM} + W_{\rm RDP}, \tag{2.5}$$

where $W_{\rm SM}$ is the radiation matrix element of the (leading-order) SM theory (see, e.g., Ref. [13]), while $W_{\rm RDP}$ is the analytical matrix element which accounts for the NLO corrections to the SM theory. In terms of the contributions $\psi_{\rm a}^{\rm SM}$ and $\psi_{\rm b}^{\rm SM}$ introduced in Eq. (2.3), the expression of $W_{\rm SM}$ correct to leading order is

$$W_{\rm SM} = W_{\rm fa,ia} + W_{\rm fa,ib} + W_{\rm fb,ia}, \tag{2.6}$$

where the subscripts indicate whether $\psi_{\rm a}^{\rm SM}$, subscript (a), or $\psi_{\rm b}^{\rm SM}$, subscript (b), are used for the initial, subscript (i), or final, subscript (f), states. The expression for $W_{\rm RDP}$ containing all terms of third order in Z/c in the cross section that survive at high energies, consists, as shown in Ref. [14], of the two contributions which consider the additional term $\psi_{\rm c}^{\rm RDP}$ in the initial, respectively final, channel,

$$W_{\rm RDP} = W_{\rm fa,ic} + W_{\rm fc,ia}, \tag{2.7}$$

following the nomenclature of Eq. (2.6). Roche *et al.* [14] managed to obtain with the help of Eq. (2.4) the following closed form,

$$\begin{aligned}
W_{\rm RDP} = &-\left[\frac{1}{k_{\rm i}^2 - (\boldsymbol{k}_{\rm f} + \boldsymbol{k})^2} + \frac{1}{k_{\rm f}^2 - (\boldsymbol{k}_{\rm i} - \boldsymbol{k})^2}\right]\\
&\times \frac{2\pi^2 Z^2}{c^2\,q}\, N_{\rm i}^{\rm SM}\, N_{\rm f}^{\rm SM}\left(u_{k_{\rm f}}^{(\sigma_{\rm f})\dagger}\,\boldsymbol{\alpha}\cdot\boldsymbol{e}_\lambda^*\, u_{k_{\rm i}}^{(\sigma_{\rm i})}\right),
\end{aligned} \tag{2.8}$$

where $\boldsymbol{q} = \boldsymbol{k}_{\rm i} - \boldsymbol{k}_{\rm f} - \boldsymbol{k}$ is the momentum transfer and $N_{\rm f}^{\rm SM}$ is analogous of $N_{\rm i}^{\rm SM}$ for the final state.

The bremsstrahlung intensity has, however, to be calculated from

$$\int d\Omega_{\rm f}\;|W_{\rm rad}|^2 \equiv \int d\Omega_{\rm f}[|W_{\rm SM}|^2 + 2{\rm Re}(W_{\rm SM}^* W_{\rm RDP})]. \tag{2.9}$$

The integrand in Eq. (2.9) differs from the absolute square of Eq. (2.5) by the term $|W_{\rm RDP}|^2$, which is one of the still higher order terms in Z/c. We recall that this term had been retained inconsistently in all earlier publications on this subject.

The second step in the analytical theory is the inclusion of screening of the point-Coulomb potential, $V_{\rm Coul}$, by the potential of the atomic electrons, $V_{\rm el}$. This is done by means of the Olsen-Maximon-Wergeland (OMW) sum rule [11] applied to the cross section $[d^2\sigma/(d\omega\,d\Omega_k)]_{\rm Coul}$, pertaining to $V_{\rm Coul}$, in order to obtain the respective cross section for the full static potential, $V = V_{\rm Coul} + V_{\rm el}$,

$$\begin{aligned}
\left(\frac{d^2\sigma}{d\omega\,d\Omega_k}\right)_{\rm screened} &= \left(\frac{d^2\sigma}{d\omega\,d\Omega_k}\right)_{\rm Coul}\\
&+\left[\left(\frac{d^2\sigma}{d\omega\,d\Omega_k}\right)_{\rm screened}^{\rm PWBA} - \left(\frac{d^2\sigma}{d\omega\,d\Omega_k}\right)_{\rm Coul}^{\rm PWBA}\right].
\end{aligned} \tag{2.10}$$

The screening correction in the second line of Eq. (2.10) is given by the difference in the PWBA cross sections with $V = V_{\rm Coul} + V_{\rm el}$ and $V = V_{\rm Coul}$, respectively. The applicability of the OMW additivity rule to the doubly differential cross section for not too low initial or final electron energies was conjectured by Olsen *et al.* [11]. This screening correction can be calculated within the PWBA, because it is only important at large electron-atom distances where the nuclear potential is considerably attenuated. A quantitative justification of the neglect of higher order terms in the PWBA is offered at the end of Sec. III.

An important simplification introduced by treating screening in the PWBA is that the effect of the potential $V_{\rm el}$, generated by the charge distribution of the atomic electrons, is completely accounted for by an atomic form factor [18]

$$F(q) = 1 + \frac{c\,q^2}{4\,\pi\,Z}\int d\boldsymbol{r}\, e^{i\boldsymbol{q}\cdot\boldsymbol{r}}\, V_{\rm el}(r). \tag{2.11}$$

We note that the replacement of the potential by its form factor is only strictly valid in the PWBA.

To establish the OMW rule, three main assumptions had to be made: (a) the relevant contributions to the radiation matrix element in Eq. (2.2) originate from the same regions of space (corresponding to $q \approx c$ and $q \approx c^3/E_{\rm i} \approx c^3/E_{\rm f}$) both for the correct result and for the PWBA, (b) the initial and final energies of the electron are high (i.e., $E_{\rm i} \gg c^2$, $E_{\rm f} \gg c^2$) so that the Wentzel-Kramers-Brillouin (WKB) approximation can be used, and (c) all involved angles are small. Moreover, Olsen *et al.* [11] adopted for $[d^2\sigma/(d\omega\,d\Omega_k)]_{\rm Coul}$ the LO-SM

expression, which is justified by the assumptions (b) and (c). Since their result is based on the WKB approximation and not on an expansion in Z/c, it holds for all Z/c. As was also shown, the OMW additivity rule is only valid for the singly and doubly differential cross section: In fact, for the triply differential one, there is an additional correction to the PWBA from the region of space where $q \approx c$. So Ref. [11] leaves open three main questions about the general validity of this prescription: (i) what is the lowest allowed collision energy, (ii) what happens at larger angles, and (iii) what happens when higher order corrections to the LO-SM theory are included.

Explicit formulas for the PWBA, the LO-SM, and the NLO-SM cross sections used in the present work can be found in Refs. [15,18]. Despite the closed-form expressions, it is still necessary to evaluate the Gauss hypergeometric function twice for each value of the triply differential cross section and to perform multidimensional integrations with adaptive Gaussian quadratures. Details about the numerical implementation and all the tests that have been performed to ensure the correctness of the developed program are reported in Ref. [19].

B. Dirac partial-wave method

In the Dirac partial-wave (DW) theory, the scattering states ψ_i and ψ_f are expanded in terms of partial waves. For each partial wave, the radial Dirac equation for an electron moving in the potential $V(r)$ is solved numerically (with the help of the code by Salvat *et al.* [20]). $V(r)$ can be obtained from the nonrelativistic Hartree-Fock density distribution of the target electrons. Koga [21] provides a representation of this density in terms of a superposition of exponentials obtained by a fitting procedure.

An advantage of the partial-wave representation is the fact that the angular integration involved in the calculation of the radiation matrix element can be performed analytically. However, the radial integrals have to be evaluated numerically [9]. In the present work, the complex-plane rotation method, introduced by Yerokhin and Surzhykov [12] into the bremsstrahlung theory to achieve convergence, is used for carrying out these integrals. Details of the formalism and of the numerical procedure can be found in Refs. [12,22].

In order to quantify screening, the calculations are repeated with the point-Coulomb field $V_\mathrm{Coul}(r)$ instead of the static potential $V(r)$. The screening effects, both in the SM and DW approaches, are gauged in terms of the ratio R_sc. This ratio is given by the difference of the respective cross sections, normalized to the result of the DW theory including screening, according to

$$R_\mathrm{sc} = \frac{d^2\sigma_\mathrm{Coul} - d^2\sigma_\mathrm{screened}}{d^2\sigma^\mathrm{DW}_\mathrm{screened}}, \tag{2.12}$$

where $d^2\sigma$ is an abbreviation for $d^2\sigma/(d\omega\, d\Omega_k)$.

It is important to stress that as long as a sufficiently large number of partial waves is included to achieve convergence, the results obtained are exact to all orders in Z/c. Thus, they can be used to benchmark the various approximations made in the analytical approaches.

III. TESTING THE OMW ADDITIVITY RULE AT LOW IMPACT ENERGIES

We start by investigating the importance of screening for a fixed photon emission angle θ_k in the forward domain and for a fixed ratio ω/E_e between the photon frequency ω and the kinetic energy E_e of the beam electron. Only small frequencies are considered for which the momentum transfer is small and hence the photon emission occurs predominantly at large electron-atom distances where the reduction of the photon intensity by the passive target electrons is substantial. The DW calculations with screening use tabulated potentials provided by Haque [23], who employed the parametrization by Koga [21]. The corresponding form factors $F(q)$, necessary in the NLO-SM approach, are obtained by an auxiliary code based on Eq. (2.11). By comparing to available nonrelativistic Hartree-Fock form factors tabulated by Hubbell *et al.* [24], it was verified that their difference is insignificant for momentum transfers up to $q \approx c$, which are relevant for the results under consideration. However, for a full consistency between the DW and the NLO-SM approaches, we have preferred to adopt here the potential by Haque for the former and the corresponding form factors obtained from Eq. (2.11) for the latter, respectively.

Figure 1 shows the cross section results related to $V_\mathrm{Coul}(r)$ and $V(r)$ from both the analytical theory [using Eqs. (2.9) and (2.10)] and from the Dirac partial-wave method for the two target atoms Sn and Pb. Two cases are selected: (i) $\theta_k = 20^\circ$ and $\omega/E_\mathrm{e} = 0.1$ and (ii) $\theta_k = 10^\circ$ and $\omega/E_\mathrm{e} = 0.2$. (For $\theta_k = 10^\circ$ and $\omega/E_\mathrm{e} < 0.2$, the DW calculations suffer from convergence problems as the angular momentum, represented by the number of required partial waves, increases both with decreasing ω and with decreasing θ_k.) Comparing Fig. 1(a) with Fig. 1(b), it can be seen that the reduction by screening is much larger for Pb than for Sn at low impact energies. The general trends of the DW results are well reproduced by the NLO-SM approach. The agreement between the two is better at lower energies. This can be understood for the unscreened case by resorting to a result by Elwert and Haug [13], who actually proved that, in the low-energy limit, the LO-SM formula turns into the exact nonrelativistic expression obtained by Sommerfeld [2], which is correct to all orders. As a matter of fact, the NLO term, which is the only part of the unscreened NLO-SM approach that requires the high-energy limit, is not important for such small angles (e.g., for Pb at $E_\mathrm{e} = 100\,\mathrm{keV}$ it is $\lesssim 2$ per mille) and does not spoil the quality of the LO result. The disagreement which appears toward $E_\mathrm{e} = 1\,\mathrm{MeV}$ between the unscreened DW and NLO-SM approaches is mostly due to a failure of the latter at high Z, to be discussed in the next section. The representation adopted in Fig. 1 is, however, not adequate to probe the OMW additivity rule because it entangles the calculation of screening with the analytical approach for a point-Coulomb field and compensations can even happen between a failure of the two contributions which result in an improvement altogether: Consider, for example, for $\theta_k = 10^\circ$ and $\omega/E_\mathrm{e} = 0.2$ the case of Sn at $E_\mathrm{e} \approx 50$ keV and of Pb at $E_\mathrm{e} \approx 100\,\mathrm{keV}$, where the screened calculations are in better agreement than the unscreened ones.

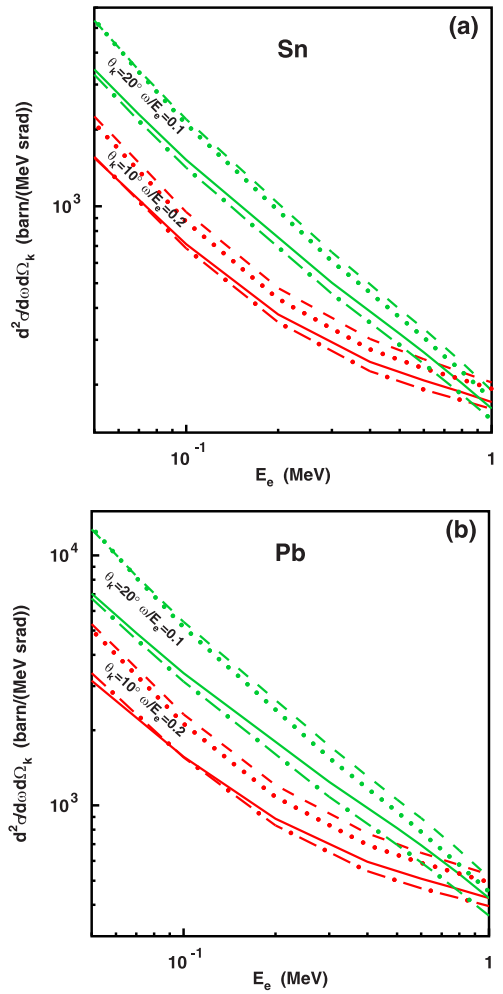

FIG. 1. Doubly differential cross section $d^2\sigma/(d\omega\, d\Omega_k)$ for bremsstrahlung emission by electron impact on (a) Sn ($Z = 50$) and (b) Pb ($Z = 82$) as a function of the initial kinetic energy E_e of the electron. Legend: − − −, point-Coulomb DW; ———, screened DW; · · · · · ·, point-Coulomb NLO-SM; and − · − · −, screened NLO-SM. Upper curves (green): $\theta_k = 20^\circ$ and $\omega/E_e = 0.1$. Lower curves (red): $\theta_k = 10^\circ$ and $\omega/E_e = 0.2$.

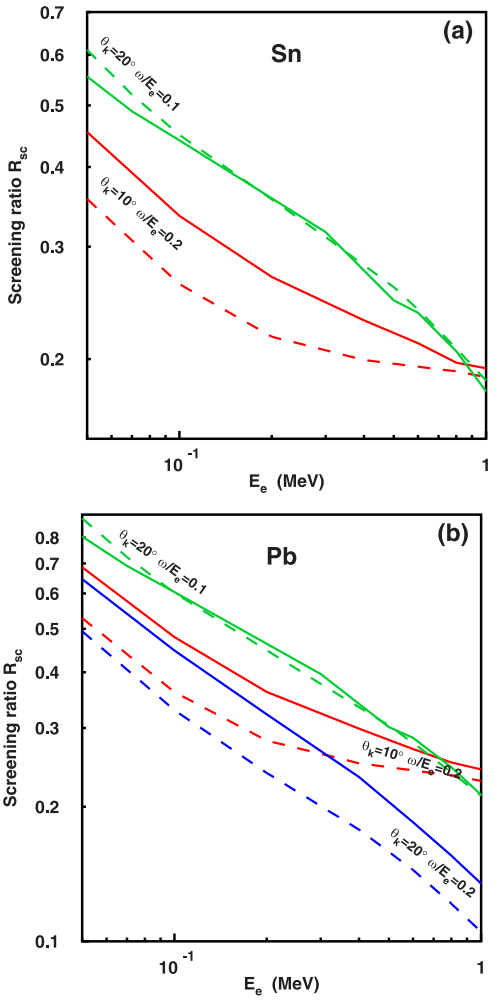

FIG. 2. Screening ratio R_{sc}^{DW} (———) and $R_{sc}^{DW,OMW}$ (− − −) according to Eq. (3.2) for bremsstrahlung from (a) Sn and (b) Pb as a function of the initial kinetic energy E_e of the electron. The results for $\theta_k = 20^\circ$ and $\omega/E_e = 0.1$ and for $\theta_k = 10^\circ$ and $\omega/E_e = 0.2$ are shown both in the upper (a) and lower (b) panels by the upper pair of curves (green) and lower pair of curves (red), respectively. In panel (b), the results for $\theta_k = 20^\circ$ and $\omega/E_e = 0.2$ are shown in addition with an even lower pair of curves (blue).

In order to disentangle the validity of the analytical approach from the validity of the OMW additivity rule, we apply the DW theory to obtain the following ratios. If the screening effects in the DW theory are accounted for by means of this rule, we get from Eq. (2.10)

$$d^2\sigma_{\rm Coul}^{\rm DW} - d^2\sigma_{\rm screened}^{\rm DW,OMW} = -\Delta\, d^2\sigma, \tag{3.1}$$

where $\Delta\, d^2\sigma \equiv d^2\sigma_{\rm screened}^{\rm PWBA} - d^2\sigma_{\rm Coul}^{\rm PWBA}$. This has to be compared with the result from the exact DW theory, $d^2\sigma_{\rm Coul}^{\rm DW} - d^2\sigma_{\rm screened}^{\rm DW}$. Normalizing with respect to $d^2\sigma_{\rm screened}^{\rm DW}$, we get for the respective ratios, according to Eq. (2.12),

$$R_{\rm sc}^{\rm DW,OMW} = \frac{-\Delta\, d^2\sigma}{d^2\sigma_{\rm screened}^{\rm DW}},$$
$$R_{\rm sc}^{\rm DW} = \frac{d^2\sigma_{\rm Coul}^{\rm DW}}{d^2\sigma_{\rm screened}^{\rm DW}} - 1, \tag{3.2}$$

which are shown in Fig. 2 for Sn and Pb.

At $\omega/E_e = 0.1$, the two ratios are much alike down to $E_e = 0.1$ MeV, for both target atoms. The ratios decrease strongly with E_e, in agreement with the expectation of diminishing screening effects [according to Eq. (2.12), $R_{\rm sc} = 0$ if screening does not occur]. However, when ω/E_e is increased to 0.2, the OMW additivity rule underestimates screening by about 30% for $E_e < 0.2$ MeV, the difference getting smaller at higher values of E_e where screening is less important.

In order to show that this feature is not due to the different choices of photon emission angle, we have studied the angular dependence of $R_{\rm sc}$ at $\omega/E_e = 0.2$ and $E_e = 0.1$ MeV for Pb up to 50°. No change in the deficiency of $R_{\rm sc}^{\rm DW,OMW}$ with angle is observed. To demonstrate this, the results for $\omega/E_e = 0.2$ and $\theta = 20^\circ$ are included in Fig. 2(b). It is seen that the difference in $R_{\rm sc}$ at lower values of E_e is much like the one for $\theta_k = 10^\circ$. The sensitivity to the value of ω/E_e indicates that the failure

of the OMW additivity rule is primarily due to the violation of the high-energy condition for the final electron. Thus, it is in general expected that the OMW prescription is not accurate for the higher part of the spectrum. However, it is important to note that, with increasing initial energy of the electron E_e, this inadequacy happens in a region where the screening itself is almost zero, so that even a large error is immaterial for the final cross section. If the cases (i) $\omega/E_e = 0.2$ and $\theta_k = 10^\circ$ and (ii) $\omega/E_e = 0.2$ and $\theta_k = 20^\circ$ are compared for collision energies beyond 300 keV, it is clear that a violation of the small-angle assumption may also lead to a failure of the OMW additivity rule. But again, with increasing initial energy of the electron, screening is small at large angles.

To analyze the behavior of our two approaches as a function of the photon frequency ω and to estimate their accuracy, we compare them with measurements [25] at an impact energy of 1 MeV. These experiments were done with foil targets thin enough so that multiple scattering and energy loss are negligibly small at photon angles above a few degrees, as analyzed in the review article by Mangiarotti and Martins [15]. Moreover, even in the worst case considered here, i.e., 1-MeV electrons emitting 0.1-MeV photons at 10°, the minimum momentum transfer is about one order of magnitude bigger than necessary to see appreciable differences between the form factors for metallic elements and free atoms (which is the case below ≈ 0.5 Å^{-1}; see, e.g., Ref. [26]). Therefore, it is safe to employ the latter.

By choosing an emission angle of 10° and increasing the photon frequency, the transition from large screening (at low ω) to insignificant screening (near the short-wavelength limit) is covered. Figure 3 shows our results for a Sn and an Au target. The DW calculations without screening are performed on a grid of points which are indicated in Fig. 3. For the lowest frequency, $\omega = 0.1$ MeV, partial-wave numbers $|\kappa_i| \leqslant 150$ and $|\kappa_f| \leqslant 130$ are required to achieve convergence in the Coulomb case, corresponding to a computation time of nearly two weeks on a conventional work station with an 800-MHz CPU. Subsequently, a spline interpolation is used to generate a continuous curve, and finally the OMW prescription is applied. The result is shown in Fig. 3 as well. The same grid is also employed for the DW calculations with screening, but only the spline interpolation is shown in the figure. The analytical approaches can be computed on a much finer mesh of about a hundred points, and therefore they can be plotted by directly joining them with segments of straight lines. For Sn [Fig. 3(a)], it is seen that the DW results using the OMW additivity rule are very close to the exact screened DW results for all frequencies. This illustrates nicely that, for $E_e \gtrsim 1$ MeV, when the OMW rule fails because the initial and final energies of the electron are not both high, screening is small and even a large error in its evaluation is not visible in the cross section. The analytical theory is somewhat lower, likewise agreeing with experiment within the error bars. This is an indication of the limitation of the NLO-SM approach for higher values of Z, discussed in the next section, where different atomic numbers and a larger angular range are studied. Similar results are found for the Au target, except that, for $\omega \gtrsim 0.5$ MeV, the analytical theory

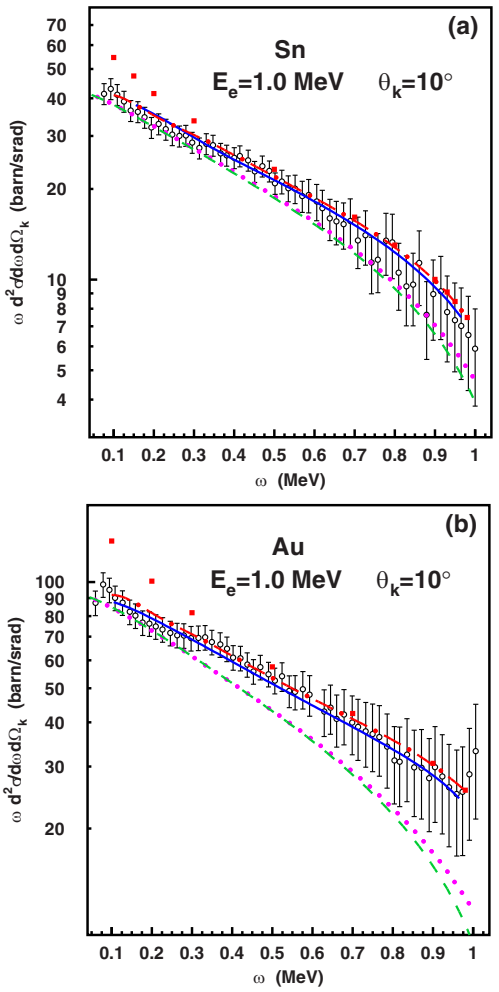

FIG. 3. Bremsstrahlung intensity $\omega\, d^2\sigma/(d\omega\, d\Omega_k)$ from 1 MeV electrons colliding (a) with Sn and (b) with Au and radiating photons at an angle of $\theta_k = 10^\circ$. Legend: ——— (blue), screened DW; ■ (red), point-Coulomb DW; — · — · — (red), point-Coulomb DW with OMW additivity rule; — — — (green), screened NLO-SM; · · · · · · (pink), screened LO-SM; and ○ (black), experimental data by Rester and Dance [25].

underestimates the DW results and experiment by up to 50%. This is a manifestation of increasing inaccuracies in the NLO-SM approach, when Z gets very large. The difference between the DW results when screening is included by means of the OMW additivity rule and the screened DW ones increases only by a small amount when proceeding from Sn to Au (the deviation grows from 0.2% for Sn to 5.1% for Au at $\omega =$ 0.15 MeV, increasing to 5.8% for Sn and 8.7% for Au near the tip), which indicates that the OMW prescription within the PWBA is rather accurate, whereas higher order terms in the Born series are obviously not relevant.

In order to check the OMW additivity rule at higher energies, we have also performed calculations within the screened DW at 2.5 MeV. For Cu at 10°, where screening is most relevant (see Fig. 4 below), the deviations between the two results at the lowest frequency investigated, $\omega = 0.5$ MeV, amount to 1.7%.

IV. VALIDITY OF THE ANALYTICAL THEORY

Having established the validity of the OMW additivity rule at $E_e = 1$ and 2.5 MeV for small angles and all frequencies, we can safely apply it in our further investigations. Figures 4–6 show photon spectra at $E_e = 2.5$ MeV and angles $10^\circ \leqslant \theta_k \leqslant 150^\circ$ for various target atoms. In these plots, all screened DW results are obtained by means of the additivity rule Eq. (2.10) after spline interpolating the calculated unscreened values, which are displayed by points. Again, the analytical approaches are computed on a fine mesh of about 120 points. The form factors tabulated by Hubbell *et al.* [24] are employed for the OMW prescription, which is applied to both the partial-wave and the analytical approaches for consistency. For Cu (Fig. 4), the lightest target investigated, the analytical NLO-SM theory is very close to the DW one up to $\theta_k = 120^\circ$,

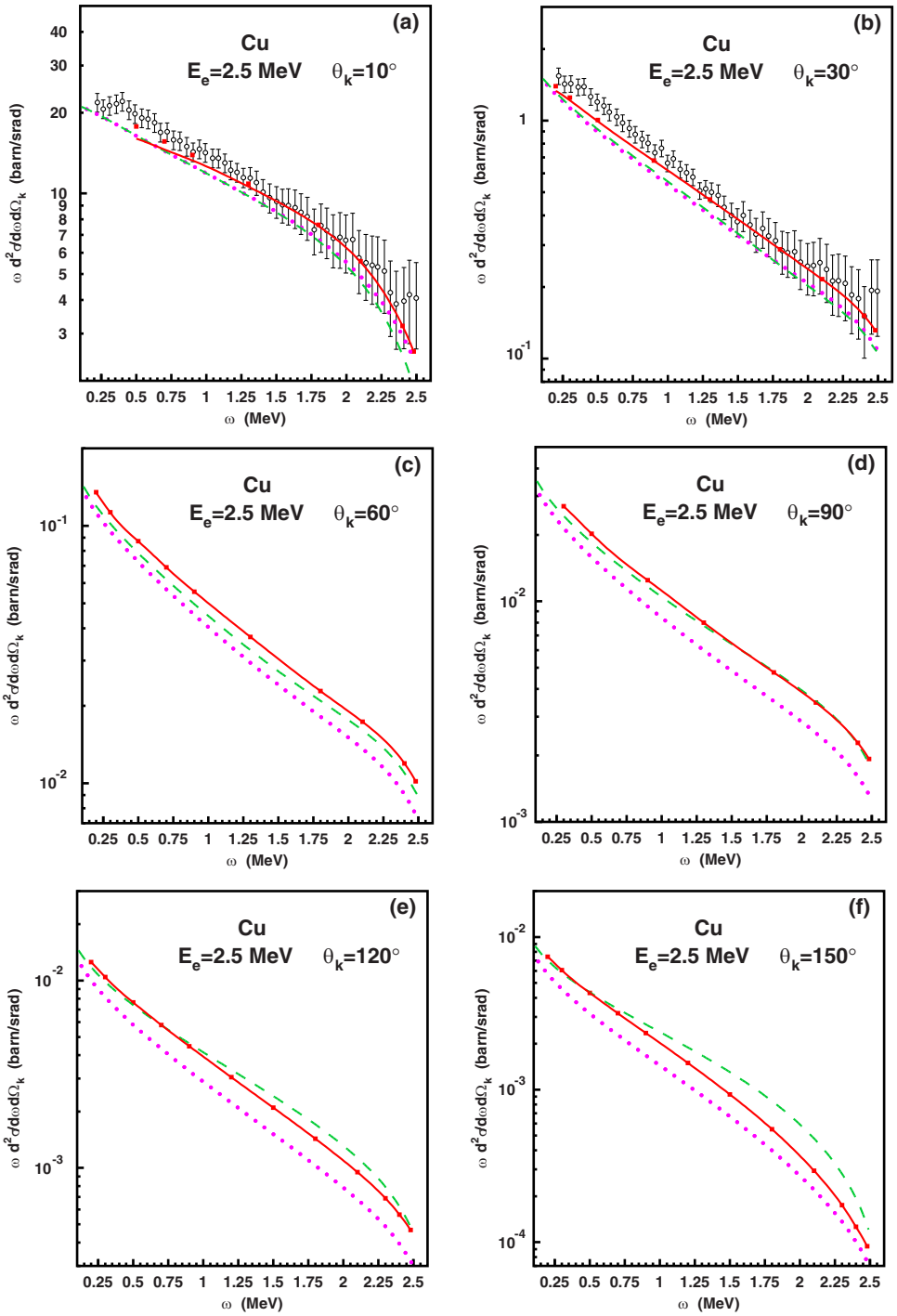

FIG. 4. Bremsstrahlung intensity $\omega\, d^2\sigma/(d\omega\, d\Omega_k)$ from 2.5-MeV electrons colliding with Cu and radiating photons at angles of (a) $\theta_k = 10^\circ$, (b) 30°, (c) 60°, (d) 90°, (e) 120°, and (f) 150° as a function of the photon frequency ω. Legend: ■ (red), unscreened DW; ——— (red), screened DW via OMW; · · · · · · (pink), screened LO-SM; — — — (green), screened NLO-SM; and ○ (black), experimental data by Rester and Dance [25].

and only at 150° it overestimates the DW results above $\omega \approx 1$ MeV. In contrast, the lowest-order SM theory gives too low cross sections already at and beyond 60°. This result is different from those of the previous works on the subject (see, e.g., Refs. [10,15,17,19]), because one still higher order term in Z/c had always been retained. Such an inconsistent prescription may hinder possible cancellation effects among all NNLO terms and gives a final result which is in severe error for backward angles, as demonstrated in Ref. [16], where results with and without this extra NNLO term are compared. Since the closed expression of the cross section found by Roche and coworkers is only valid at high electron energies,

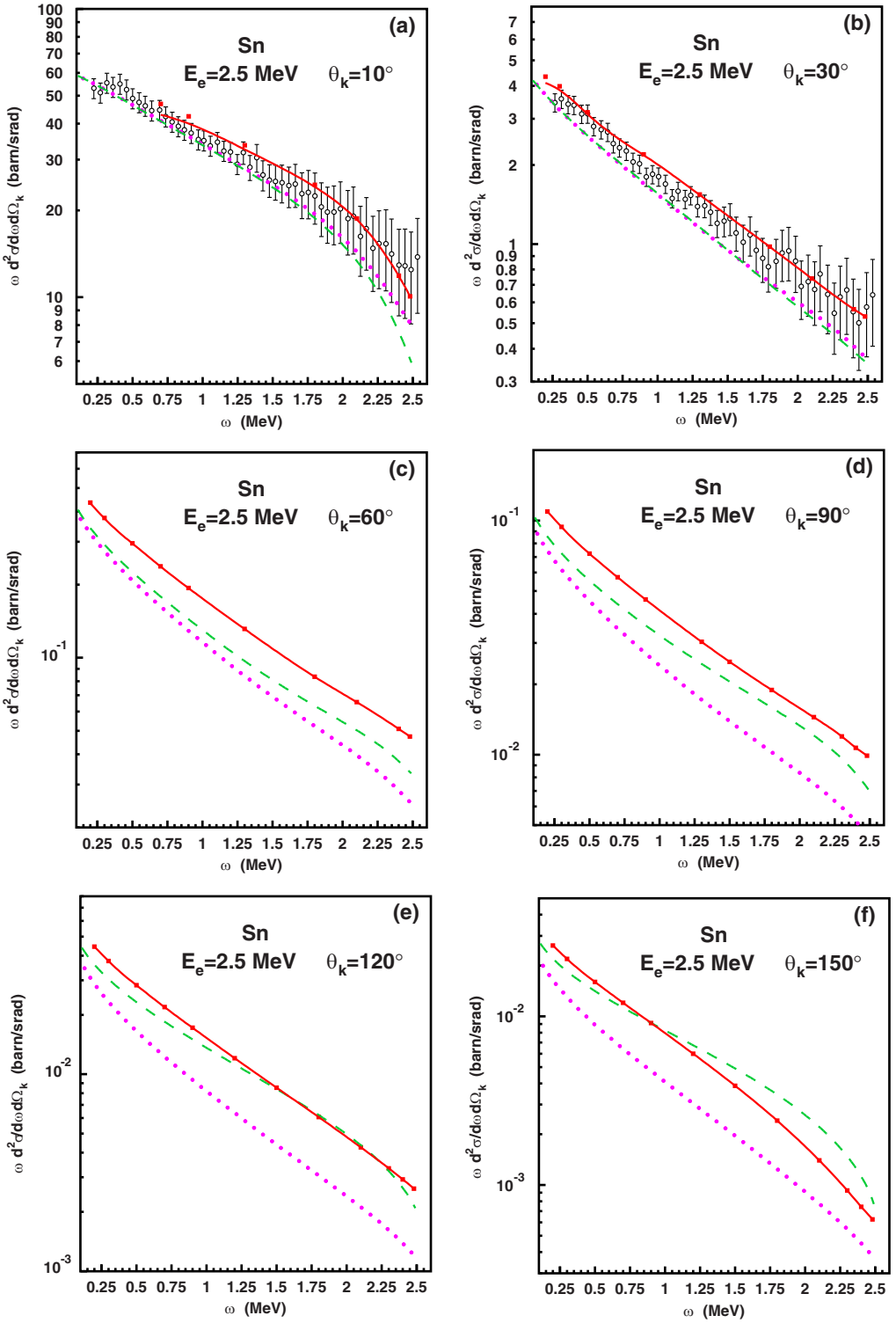

FIG. 5. Bremsstrahlung intensity $\omega\, d^2\sigma/(d\omega\, d\Omega_k)$ from 2.5-MeV electrons colliding with Sn and radiating photons at angles of (a) $\theta_k = 10°$, (b) 30°, (c) 60°, (d) 90°, (e) 120°, and (f) 150° as a function of the photon frequency ω. For the legend, see Fig. 4.

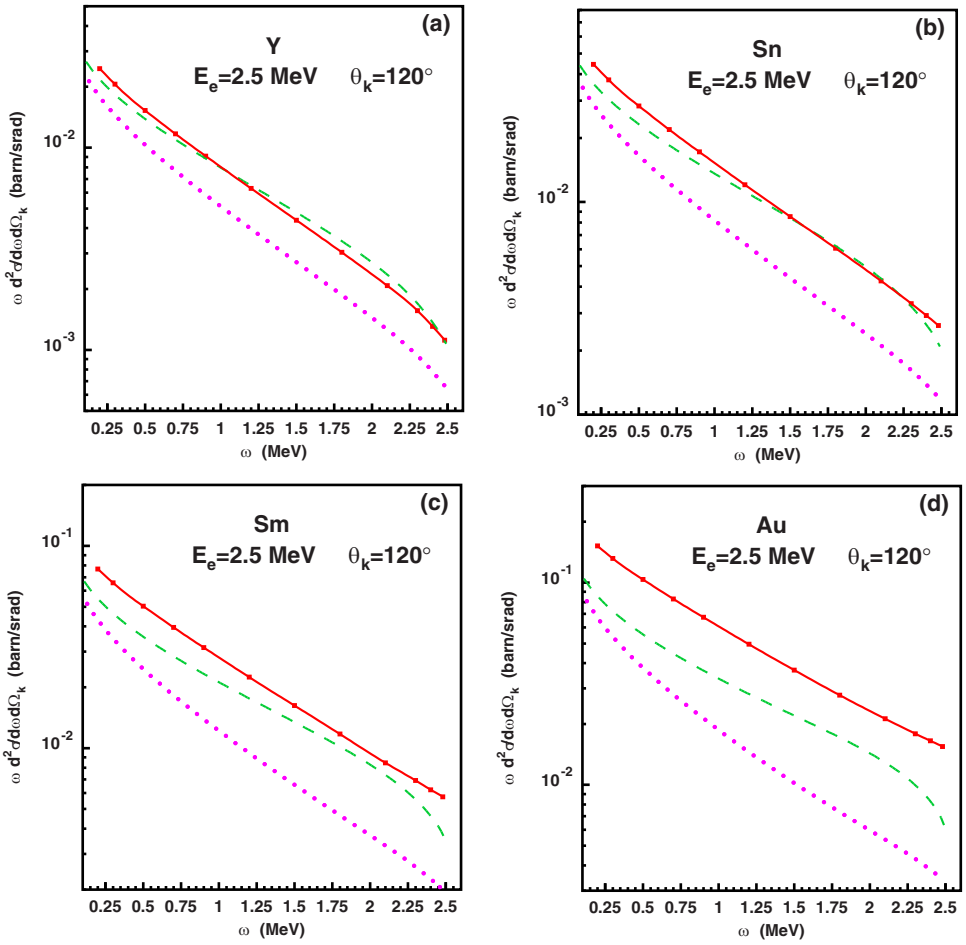

FIG. 6. Bremsstrahlung intensity $\omega\, d^2\sigma/(d\omega\, d\Omega_k)$ from 2.5-MeV electrons colliding with (a) Y, (b) Sn, (c) Sm, and (d) Au and radiating photons at an angle of $\theta_k = 120^\circ$ as a function of the photon frequency ω. For the legend, see Fig. 4.

the calculations are expected to fail in the vicinity of the short-wavelength limit (tip) where the electron is left with a small kinetic energy. Indeed, this is observed in Fig. 4 for $\theta_k = 10^\circ$, where the NLO correction, when compared to the LO-SM result, actually worsens the agreement with the DW results and the measurements close to the tip. This limitation of the NLO-SM theory is hard to perceive in the linear plots of Ref. [16]. For $\theta_k = 30^\circ$, the NLO term has no effect and above this angle it always improves the LO-SM up to the tip region (even if, in principle, there is no reason for it to work close to the short-wavelength limit). It should also be noted that screening effects are only important at the lowest frequencies and at angles $\theta_k \lesssim 30^\circ$, but are absent at all higher angles as follows from the comparison between the Coulombic and the OMW-corrected DW results.

Proceeding to the heavier element, Sn (Fig. 5), the deviations between the NLO-SM and the DW results are larger for the smaller angles, being similar to the ones for Cu at $\theta_k = 120^\circ$ and 150°. When the photon emission angle increases, the average momentum transfer q is larger. Thus, the region of space which gives the dominant contribution to the radiation matrix element Eq. (2.2) or, in the semiclassical language of the Weizsäcker-Williams approach, the relevant electron-nucleus distance at which the photon is emitted, $r \approx 1/q$, is located closer to the nucleus, such that the distortion by the Coulomb field is stronger. Since the SM wave functions are less accurate for higher Z and close to the nucleus, this leads to a genuine failure of the LO-SM theory at larger angles. Correspondingly, the NLO correction gets more important and, in turn, less precise: As in every expansion, the NLO term can be trusted as long as it is a small correction to the LO one. However, a fundamental property of the SM wave functions, when using them for calculating bremsstrahlung cross sections, is that they are always a good approximation to the exact ones, irrespective of Z, if the photon emission is simultaneously close to the direction of both the initial and final momentum of the electron [7]. This property renders the LO-SM cross sections very accurate at high energies and low θ_k for all Z, since the final angles of the electron contributing significantly to Eq. (2.1) are indeed small. This is confirmed for $\theta_k = 10^\circ$ and 30°, where the LO result agrees with the data within the experimental uncertainty. By using the DW results as a guide for the correct behavior close to the tip (where the spread of the experimental points increases due to the reduction in statistics), it is evident that there the LO-SM fails at all angles. Actually, for small final energies of the electron, larger final angles of the electron can contribute to Eq. (2.1), which worsen the accuracy of the LO-SM approach. Like for Cu, the NLO term increases the inaccuracy of the LO result for $\theta_k = 10^\circ$ close to the tip, being worse for Sn

TABLE I. Deviation of the doubly differential cross section for bremsstrahlung calculated with the LO-SM and NLO-SM approaches with respect to the ones obtained by the DW method and corrected for screening with the OMW additivity rule. The case considered is that of electrons with $E_e = 2.5\,\mathrm{MeV}$ impinging on Cu, Y, Sn, Sm, and Au and radiating photons at the indicated θ_k angle. To get a single value, a maximum has been taken over the photon energies $\omega \leqslant 2.5\,\mathrm{MeV}$ for $\theta_k > 30^\circ$ and over $\omega \leqslant 1.5\,\mathrm{MeV}$ for $\theta_k \leqslant 30^\circ$. The calculations are the same as employed for Figs. 4–6.

θ_k [deg]	Cu [%]	Y [%]	Sn [%]	Sm [%]	Au [%]
		LO-SM			
10	8.8		16		
30	14		26		
60	26		46		
90	31		53		
120	32	41	54	65	78
150	29		50		
		NLO-SM			
10	9.2		18		
30	13		26		
60	11		29		
90	10		27		
120	20	14.5	19	35	57
150	63		60		

than for Cu. For $\theta_k = 30^\circ$, this effect is minimized, whereas for larger angles, the NLO-SM theory improves the LO-SM theory.

The angle $\theta_k = 120^\circ$, where for Sn our two theories agree best, has been selected to study the photon spectrum for other targets including yttrium ($Z = 39$), samarium ($Z = 62$), and gold ($Z = 79$), as shown in Fig. 6. While for $Z \leqslant 50$ the NLO-SM and DW results are very close at this angle, they start to differ for the heavier atoms, particularly for Au, by up to a factor of 2. However, these results clearly demonstrate the improvement over the LO-SM theory when the next-to-leading-order terms in Z/c are retained. In particular, the behavior with Z is smooth and monotonic. This contrasts the results of the inconsistent analytical theory used in previous works; for example, compare Sn and Au at $E_e = 1.7\,\mathrm{MeV}$ and $\theta_k = 60^\circ$ in Fig. 1 of Ref. [17] or Sn and Au at $E_e = 2.5\,\mathrm{MeV}$ and $\theta_k = 30^\circ$ in Fig. 6 of Ref. [19], where the higher order correction is bigger for the lower Z element.

To summarize in a quantitative way Figs. 4–6, the maximum deviations of the LO-SM and NLO-SM results with respect to the DW ones, accounting for screening by means of the OMW additivity rule, are reported in Table I. Because of the limitations discussed above, for $\theta_k = 10^\circ$ and 30°, only the part of the spectrum below 1.5 MeV is considered to evaluate the largest error. Except for the smallest and largest angles ($\theta_k = 10^\circ$ and 150°), the positive effect of the NLO correction is rather clear. Excluding $\theta_k = 150^\circ$ and $\omega > 1.5\,\mathrm{MeV}$ for $\theta_k = 10^\circ$ and 30°, the errors are between 10% and 20% for Cu, rising to 20–30% for Sn. For Au, where only $\theta_k = 120^\circ$ is probed, it reaches nearly 60%.

V. CONCLUSIONS

In this work, doubly differential cross sections for bremsstrahlung emission in the collision of electrons with a series of neutral target atoms are considered. Two theoretical approaches are used, the analytical NLO-SM theory (accurate to third order in Z/c at high energies) and the numerical DW theory (exact to all orders).

By comparing for small frequencies and forward photon emission angles the DW theory, with an exact account of screening, with the results obtained from the point-Coulomb DW ones with the help of the Olsen-Maximon-Wergeland additivity rule, it has been shown that such a prescription can be applied when the initial and final energies of the electron are both not small and when the photon is emitted into forward directions. Notably, the rule works even down to beam energies of $E_e = 100\,\mathrm{keV}$, provided the photon frequency is very low as compared to E_e and the photon angle is small. However, for $E_e \gtrsim 1\,\mathrm{MeV}$, the conditions where the rule holds are just the ones where screening is appreciably different from zero. This results in a general applicability for all frequencies and emission angles.

A comparison between the NLO-SM and the DW results for larger angles has revealed that at impact energies as low as 2.5 MeV the SM-based theory gives quantitative results even for the heaviest elements at all photon angles up to at least 120° (the maximum deviations being between 10% and 20% for Cu, rising to 20–30% for Sn, and up to 60% for Au). The exception is a small frequency interval near the short-wavelength limit, where a SM function for the slow scattered electron is bound to fail if Z is large. We could also demonstrate that the NLO-SM approach improves considerably on the (lowest-order) Sommerfeld-Maue theory for the larger angles.

ACKNOWLEDGMENTS

D.H.J. would like to thank A.K.F. Haque for providing the static potentials for Cu, Sn, Au, and Pb. A.M. would like to acknowledge support from Fundação de Amparo à Pesquisa do Estado de São Paulo (FAPESP) under Contracts No. 2013/15634-5 and No. 2016/13116-5, from Conselho Nacional de Desenvolvimento Científico e Tecnológico (CNPq) under Contract No. 306331/2016-0, and from Universidade de São Paulo under Programa Institucional de Apoio aos Novos Docentes Process No. 17.1.9256.1.4.

[1] B. Rossi, *High-Energy Particles* (Prentice Hall, New York, 1952).
[2] A. Sommerfeld, Ann. Phys. **11**, 257 (1931).
[3] F. Sauter, Ann. Phys. **20**, 404 (1934).
[4] H. A. Bethe and W. Heitler, Proc. R. Soc. London, Ser. A **146**, 83 (1934).
[5] H. A. Bethe, Proc. Camb. Philos. Soc. **30**, 524 (1934).
[6] G. Racah, Nuovo Cimento **11**, 461 (1934).

[7] H. A. Bethe and L. C. Maximon, Phys. Rev. **93**, 768 (1954).
[8] A. Sommerfeld and A. W. Maue, Ann. Phys. (Leipzig) **22**, 629 (1935).
[9] H. K. Tseng and R. H. Pratt, Phys. Rev. A **3**, 100 (1971).
[10] A. Mangiarotti and D. H. Jakubassa-Amundsen, Phys. Rev. A **96**, 042701 (2017).
[11] H. Olsen, L. C. Maximon, and H. Wergeland, Phys. Rev. **106**, 27 (1957).
[12] V. A. Yerokhin and A. Surzhykov, Phys. Rev. A **82**, 062702 (2010).
[13] G. Elwert and E. Haug, Phys. Rev. **183**, 90 (1969).
[14] G. Roche, C. Ducos, and J. Proriol, Phys. Rev. A **5**, 2403 (1972).
[15] A. Mangiarotti and M. N. Martins, Radiat. Phys. Chem. **141**, 312 (2017).
[16] A. Mangiarotti, D. H. Jakubassa-Amundsen, and M. N. Martins, Radiat. Phys. Chem. (2019).
[17] A. Mangiarotti and M. N. Martins, Phys. Rev. A **94**, 022708 (2016).
[18] E. Haug and W. Nakel, *The Elementary Process of Bremsstrahlung* (World Scientific, Singapore, 2004).
[19] A. Mangiarotti, M. N. Martins, and V. R. Vanin, Nucl. Instrum. Methods Phys. Res. B **446**, 58 (2019).
[20] F. Salvat, J. M. Fernández-Varea, and W. Williamson Jr., Comput. Phys. Commun. **90**, 151 (1995).
[21] T. Koga, Theoret. Chim. Acta **95**, 113 (1997).
[22] D. H. Jakubassa-Amundsen, Phys. Rev. A **93**, 052716 (2016).
[23] A. K. F. Haque (private communication); see also A. K. F. Haque *et al.*, J. Phys. Commun. **2**, 125013 (2018).
[24] J. H. Hubbell, W. J. Veigele, E. A. Briggs, R. T. Brown, D. T. Cromer, and R. J. Howerton, J. Phys. Chem. Ref. Data **4**, 471 (1975); **6**, 615(E) (1977).
[25] D. H. Rester and W. E. Dance, Phys. Rev. **161**, 85 (1967).
[26] M. A. Tabbernor, A. G. Fox, and R. M. Fisher, Acta Cryst. A **46**, 165 (1990).